

Some analytical results for the velocity of cracks propagating in nonlinear lattices

T. M. Guozden and E. A. Jagla

Centro Atómico Bariloche, Comisión Nacional de Energía Atómica (8400) Bariloche, Argentina

(Received 31 March 2006; published 14 July 2006)

We analyze a piecewise linear elastic model for the propagation of a crack in a stripe geometry under mode III conditions, in the absence of dissipation. The model is continuous in the propagation direction and discrete in the perpendicular direction. The velocity of the crack is a function of the value of the applied strain. We find analytically the value of the propagation velocity close to the Griffith threshold, and close to the strain of uniform breakdown. Contrary to the case of perfectly harmonic behavior up to the fracture point, in the piecewise linear elastic model the crack velocity is lower than the sound velocity, reaching this limiting value at the strain of uniform breakdown. We complement the analytical results with numerical simulations and find excellent agreement.

DOI: [10.1103/PhysRevE.74.016106](https://doi.org/10.1103/PhysRevE.74.016106)

PACS number(s): 46.50.+a, 62.20.Mk

I. INTRODUCTION

The velocity of a crack propagating in a brittle material is known to be related to the sound velocity in the material. This general statement can be qualitatively justified by noticing that a crack is a sort of elastic disturbance, although of course of extreme nonlinear nature. Thus it is not surprising that its velocity is related to the velocity of propagation of small amplitude elastic deformations. However, when we want to be more precise about the relation between crack velocity and sound velocity, difficulties appear. In textbook treatments of linear elastic fracture mechanics, it is suggested that the maximum crack velocity is given by the Rayleigh velocity v_R [1,2]. This limit is expected to be achieved at large driving forces (i.e., large applied strain), since for low driving forces the discrete (atomic) nature of the material may reduce the velocity drastically (this is called the lattice trapping effect). Experimentally, an increase of the velocity with the applied strain is observed in general, however, the limiting Rayleigh velocity is almost never achieved [3]. Microscopical observations of crack paths in different kinds of samples reveal one source of this discrepancy: at velocities roughly close to $v_R/3$ a straight crack path destabilizes, becoming wandering, and generating side branches at larger velocities. Some people have claimed [4] that if this effect is taken into account (i.e., the true microscopic crack path length is larger than the apparent macroscopic length) then the classical prediction is verified. But this cannot be claimed to be always the case [5]. Even restricting to cracks propagating in a stationary fashion along a perfectly linear path, a careful analysis reveals that crack propagation velocity cannot be determined independently of the microscopic details close to the crack tip [1,2]. This means that a purely macroscopic analysis using continuous approximations for the material leaves the velocity of the crack undetermined. This is the reason why detailed models of the breaking phenomena at the atomic scale are necessary in determining crack velocities.

A class of fully consistent models on which crack velocities can be calculated (albeit numerically) are lattice spring models where the material is represented by a set of point masses joined by springs [6]. These springs can break when

some threshold deformation is reached giving rise to cracks in the form of connected sets of broken springs.

It has been recently established [7,8] that the propagation velocity in this kind of model crucially depends on the presence of anharmonicities of the springs. These anharmonicities are also called hyperelastic effects. The most spectacular case is that of hyperelastic stiffening (i.e., springs becoming stiffer at large deformation), that can produce supersonic crack propagation, something that had been considered impossible in classical treatments of fracture. However, the case of hyperelastic softening is by far the expected most common case, since most decohesion potentials typically interpolate smoothly between the weakly deformed material and the broken material, in which the elastic constants are formally zero. In this case, and even in the absence of other effects such as crack velocity oscillation or crack branching, hyperelastic softening produces a noticeable reduction of the crack velocity.

Even in the relatively simple class of lattice spring models, quantitative predictions of crack velocity is elusive, since, as already stated, breaking of the material is a form of nonlinear behavior, and it is typically very difficult to find exact results for nonlinear models. The situation is even worse in the presence of hyperelasticity, which is an additional source of nonlinear behavior.

In this paper we show that taking a continuous approximation in the propagation direction in a class of lattice spring models, some exact results can be obtained for the crack velocity even in the presence of hyperelastic softening. These results shed light on the effect of hyperelasticity on crack propagation, and serve as a starting point for other (most likely numerical) studies in more realistic models.

We have also implemented the model numerically and compared the simulated results with the analytical ones, finding excellent agreement.

II. THE MODEL

We consider a lattice spring model in a stripe geometry with fixed displacement mode III boundary conditions. A continuous description is implemented in the propagating direction (along the stripe, chosen to be the x direction),

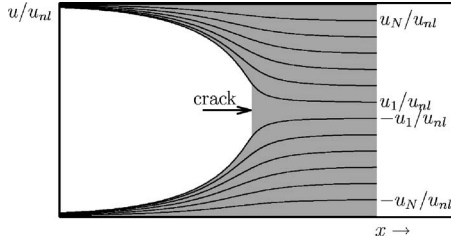


FIG. 1. A sketch of the model studied: a set of $2N$ continuous nonlinear elastic chains (represented by the continuous lines) are coupled through perfectly harmonic interactions if the separation between chains is lower than a threshold value u_{bk} (shaded region). If this value is exceeded (this may occur only between chains u_1 and $-u_1$) the two chains decouple defining the crack. In the figure, intact springs are shadowed. The crack advances to the right as the system evolves. Boundary conditions are fixed displacements imposed at the top and bottom of the figure.

whereas a discrete model is considered in the perpendicular (y) direction. Thus the model consists of a set of a fixed number ($2N$) of continuous elastic (unbreakable) chains as depicted in Fig. 1. Taking into account the symmetry of the system, we solve the equations only for the upper half of it, in which each chain is labeled by a discrete index j , $1 \leq j \leq N$. We consider the (out of plane) mode III displacement of the chains, that is noted $u_j(x)$ for chain j . Chain j is coupled to the two neighbor chains by harmonic springs. These springs can break when the coordinate difference between chains is larger than a breaking threshold that we note u_{bk} , giving rise to a “crack” propagating in the system. We will always assume that the crack propagates in the middle of the stripe, i.e., between chains u_1 and $-u_1$, as indicated in Fig. 1. Our aim is to find the stable propagation velocity of this crack. Chains u_N and $-u_N$ are coupled to the lateral sides of the system, on which fixed displacements are applied. The sides of the system can be formally introduced as chains u_{N+1} (and $-u_{N+1}$), with $u_{N+1}(x) = (N+1/2)\delta$. This defines δ as the nominal strain in the system. Hyperelasticity comes from the assumption that the spring constant of a chain changes from a low stretching value k_0 when $|du_j(x)/dx| < u_{nl}$, to a value $k_0\gamma$ when $|du_j(x)/dx| > u_{nl}$. Thus u_{nl} can be appropriately called the nonlinear threshold of the chains. In the present paper we consider only the case of hyperelastic softening, namely $\gamma < 1$. In short, the model is defined by the equation:

$$\rho \frac{d^2 u_j}{dt^2} = k_0 \eta (du_j/dx) \frac{d^2 u_j}{dx^2} + \nu (u_{j+1} - u_j) + \nu (u_{j-1} - u_j) \quad (1)$$

with the functions η and ν defined as follows:

$$\begin{aligned} \eta(y) &= 1 & \text{if } |y| < u_{nl}, \\ \eta(y) &= \gamma & \text{if } |y| > u_{nl}, \\ \nu(y) &= y & \text{if } |y| < u_{bk}, \\ \nu(y) &= 0 & \text{if } |y| > u_{bk}, \end{aligned} \quad (2)$$

where ρ is the linear density of each chain and the interchain harmonic spring constant is taken as unity.

We want to obtain the solution to this equation when the external strain δ is in between two limiting values. The lowest possible value for propagation corresponds to the Griffith’s threshold δ_G , at which the elastic energy available in the system ahead of the crack equals that stored in the broken springs behind the crack. An easy calculation shows that $\delta_G = u_{bk}/\sqrt{2N+1}$. On the other hand the maximum external strain that can be supported by the system is the one that would break the system even in the absence of any pre-existent crack. Clearly the strain for uniform breaking δ_U is given by $\delta_U = u_{bk}$.

A few remarks are in order. Our model is obviously anisotropic, as there are continuous chains along the x direction, whereas the system is discrete in the y direction. Another source of anisotropy lies in the fact that hyperelastic softening is introduced only inside the chains, but not in the interchain springs. We have previously indicated [8] that in fact it is the hyperelasticity in the propagation direction that drives the nontrivial evolution of the system. There is no point in introducing hyperelasticity in the interchain springs, as this has no important effect in the dynamics and complicates greatly the analytical treatment. Note also that chains are not allowed to break, it is only the vertical interchain springs that break. This forces the crack to remain in the center of the stripe and avoids effects such as crack branching.

The wave velocity inside each chain is given by $V_w \equiv \sqrt{k_0/\rho}$. In the highly stretched case, the spring constant changes in a factor of γ (we always take $\gamma < 1$), so we can define the stretched wave velocity V_w^γ as $V_w^\gamma = \sqrt{k_0\gamma/\rho}$. We will solve the model under the assumption that there is a stable propagation of a crack in the middle of the stripe, with a velocity V . As we will see, this velocity—if not zero—will never be larger than V_w , nor lower than V_w^γ .

III. SCALING PROPERTIES OF THE SOLUTION

Before presenting the analytical results we have derived, it is interesting to indicate some constraints on the solution that can be obtained using scaling arguments only. Let us suppose we have obtained the solution $u_j(x, t)$ corresponding to a given set of parameters u_{nl} , u_{bk} , γ , and some applied strain δ , and that this solution has a velocity V . It is then immediate to verify that a rescaled solution αu is also a solution of the problem for an applied strain $\alpha\delta$, with the same velocity V if the parameters u_{bk} and u_{nl} are rescaled to αu_{bk} and αu_{nl} . This means that the velocity can be written as a function of the combinations u_{bk}/u_{nl} , and δ/u_{nl} .

A less trivial scaling can be obtained by changing a solution of the form $u(x, t)$, to a new form $w(x, t) \equiv u(Ax, Bt)$, and finding A and B and new coefficients of the model for $w(x, t)$ to be a solution. The calculation is straightforward, and we present only the result, that can be stated as the fact that the velocity of the crack should be of the form

$$\sqrt{1 - \left(\frac{V}{V_w}\right)^2} = \sqrt{1 - \gamma} f\left(N, \frac{\delta}{u_{nl}\sqrt{1-\gamma}}, \frac{u_{bk}}{u_{nl}\sqrt{1-\gamma}}\right), \quad (3)$$

where f is an undetermined function of the arguments and where we also made use of the previously obtained scaling.

Already from this scaling relation a very important result can be obtained. This corresponds to the case in which there is no hyperelastic softening, i.e., in which the spring constants within the chains remain always equal to k_0 . This can be formally obtained by letting u_{nl} go to infinity. Then the right-hand side of Eq. (3) becomes $\sqrt{1-\gamma}f(N,0,0)$. Since obviously in this limit the crack velocity cannot depend on γ , the only possibility is that $f(N,0,0)=0$, which implies $V=V_w$. This means that in the absence of hyperelastic effects the crack velocity is equal to the wave velocity for any $\delta > \delta_G$.

IV. EXACT SOLUTION FOR $N=1$

We present here the exact analytic solution of the previous nonlinear model in the case $N=1$. This will be a reference result for the further discussion of the more interesting cases with $N > 1$.

Assuming a stationary propagation, we define the stationary solution $\tilde{u}(x) \equiv u_1(x-Vt, t=0)$, where V is the propagation velocity to be determined self-consistently. We choose the reference system in such a way that the crack tip is located at $x=0$. Thus, we must search for solutions of the piecewise defined equation (we eliminate the tilde for simplicity):

$$\left[1 - \left(\frac{V}{V_w} \right)^2 \right] \frac{d^2 u}{dx^2} = u - \frac{3\delta}{2}; \quad x < 0, \quad \left| \frac{du}{dx} \right| < u_{nl}, \quad (4)$$

$$\left[1 - \left(\frac{V}{V_w} \right)^2 \right] \frac{d^2 u}{dx^2} = 3u - \frac{3\delta}{2}; \quad x > 0, \quad \left| \frac{du}{dx} \right| < u_{nl}, \quad (5)$$

$$\left[\gamma - \left(\frac{V}{V_w} \right)^2 \right] \frac{d^2 u}{dx^2} = u - \frac{3\delta}{2}; \quad x < 0, \quad \left| \frac{du}{dx} \right| > u_{nl}, \quad (6)$$

$$\left[\gamma - \left(\frac{V}{V_w} \right)^2 \right] \frac{d^2 u}{dx^2} = 3u - \frac{3\delta}{2}; \quad x > 0, \quad \left| \frac{du}{dx} \right| > u_{nl}, \quad (7)$$

with the additional condition to be satisfied at the crack tip: $u(0) = u_{bk}/2$.

Nontrivial solutions of this nonlinear equation of motion can be obtained by matching the solution in the different regions. It can be shown in general that the crack tip (located at $x=0$) must also be the point that separates low and high stretching regions, i.e., $|du/dx| < u_{nl}$ for $x > 0$, and $|du/dx| > u_{nl}$ for $x < 0$. In fact, according to the differential equation, when the nonlinear threshold is reached, there is a change of sign in the pre-factor of d^2u/dx^2 , that passes from $[1 - (V/V_w)^2]$ to $[\gamma - (V/V_w)^2]$. But d^2u/dx^2 cannot change sign, otherwise the first derivative du/dx would be an extreme at that point, and this is inconsistent since we assumed $|du/dx| < u_{nl}$ to the right and $|du/dx| > u_{nl}$ to the left. Then the change of sign of the pre-factor of d^2u/dx^2 must be compensated by a change of sign on the right-hand side of the equation, and this is only possible at the point where the

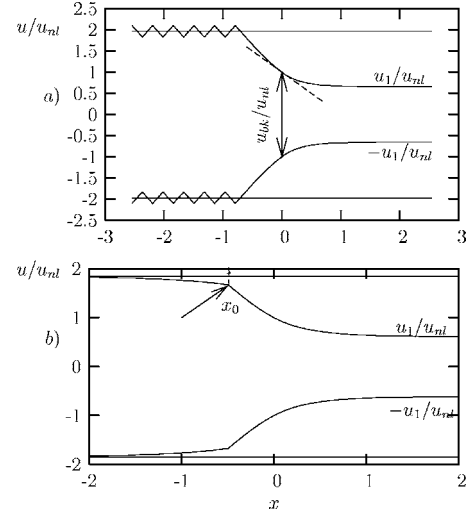


FIG. 2. Exact solutions for $N=1$, $u_{bk}/u_{nl}=2$, and $\delta/u_{nl}=1.31$ in (a) and $\delta/u_{nl}=1.23$ in (b). Jumps of $\frac{du_1}{dx}$ in (a) satisfy a momentum conservation condition given by Eq. (11). In (b), the jump in $\frac{du_1}{dx}$ at $x=x_0$ is described by Eq. (13). In this case, only the portion of chains between $x=x_0$ and $x=0$ is in the hyperelastic regime. In both cases $\frac{du_1}{dx}|_{x=0} = -u_{nl}$ and $u_1(0) = \frac{u_{bk}}{2}$.

system is breaking and the right-hand side changes from $3u - 3\delta/2$ to $u - 3\delta/2$. This justifies our statement that exactly at the crack tip, the value of $|du/dx|$ is u_{nl} .

For $x > 0$ the solution of the differential equation has the form

$$u(x) = \frac{\delta}{2} - \left(\frac{\delta}{2} - \frac{u_{bk}}{2} \right) \exp \left[- \frac{x\sqrt{3}}{\sqrt{1 - (V/V_w)^2}} \right], \quad (8)$$

where we have already used the constraint $u(0) = u_{bk}/2$, and from the requirement $|du/dx|_{x=0} = u_{nl}$ we get the velocity

$$V(\delta) = V_w \sqrt{1 - \frac{3}{4} \left(\frac{u_{bk} - \delta}{u_{nl}} \right)^2}. \quad (9)$$

Note that the velocity is independent of the value of γ , and that it is consistent with Eq. (3), as it must be. We also see explicitly that $V=V_w$ if $u_{nl} \rightarrow \infty$. To check that this is a consistent solution, we must verify that there is a reasonable form of $u(x)$ for $x < 0$.

When δ is large enough, the solution for $x < 0$ consists of a concatenation of similar pieces of the form

$$u(x) = \frac{3\delta}{2} + \frac{u_{bk} - 3\delta}{2} \cos \left(\frac{x}{\sqrt{(V/V_w)^2 - \gamma}} \right) - u_{nl} \sqrt{(V/V_w)^2 - \gamma} \sin \left(\frac{x}{\sqrt{(V/V_w)^2 - \gamma}} \right). \quad (10)$$

This kind of solution is sketched in Fig. 2(a). When two pieces of this form are matched together, the derivative of u has a jump. A momentum conservation condition must be satisfied at those points. In fact, the integral of the force on an infinitesimal piece of chain during the time in which it passes through the singular point, must be equal to the

change of momentum. It is obtained that this conservation requires that the derivative of u has a jump. The norm of the derivative is equal on both sides, and its value is

$$|du/dx| = u_{nl}(1 - \gamma)/[(V/V_w)^2 - \gamma]. \quad (11)$$

Note in Fig. 2(a) how the sort of triangular oscillation extends to $x \rightarrow -\infty$, i.e., the excess of elastic energy in the system remains in the form of kinetic and elastic energy far behind the crack tip.

When δ is reduced, the amplitude of the oscillation described by Eqs. (10) and (11) reduces also, and it vanishes at a particular value of δ . For δ values lower than this, the previous solution is not valid. It turns out that in this case the solution for $x < 0$ is singular in our continuous system. A way to “regularize” this singular solution is to consider the continuous chain as the limit of a discrete chain of point masses. When the number of masses per unit length goes to infinity, we can describe the solution that is obtained in the following way [see Fig. 2(b)]: there is a region for $x_0 < x < 0$ in which the solution has the previous form given in Eq. (10). The value $|x_0|$ depends on δ , going to 0 when $\delta \rightarrow \delta_G$ and reaching a maximum value of order 1. For $x < x_0$, the solution returns to the linear regime, and is composed by a smooth part and a singular part. The singular part is an oscillation that has an amplitude which goes to zero in the continuum limit, but a frequency that diverges in this limit, in such a way that it can carry (in the form of kinetic energy) the excess of elastic energy in the system. The regular part has the form

$$u(x) = \frac{3\delta}{2} - \left(\frac{3\delta}{2} - \frac{u_{bk}}{2} \right) \exp \left[\frac{x\sqrt{2}}{\sqrt{(V/V_w)^2 - \gamma}} \right], \quad (12)$$

and the matching conditions at x_0 for this regular part correspond to have continuity of the function, i.e., $u(x_0^-) = u(x_0^+)$, and a jump in the derivative given by

$$[1 - (V/V_w)^2] \left. \frac{du}{dx} \right|_{x_0^-} - [\gamma - (V/V_w)^2] \left. \frac{du}{dx} \right|_{x_0^+} = u_{nl}(1 - \gamma) \quad (13)$$

which is obtained using the same kind of conservation arguments that led to Eq. (11). In Sec. VI we will show results of numerical simulations that confirm and clarify further this behavior.

We see in the solution for $x < 0$ [Eq. (10)] that when $V \rightarrow V_w^\gamma$ the frequency of the oscillation for $x < 0$ diverges. In fact, if according to Eq. (9) the velocity would be lower than V_w^γ , then neither the solutions given by Eq. (10) nor Eq. (12) exist. It can be shown that in this case the velocity of crack propagation is actually $V = V_w^\gamma$. This regime is not particularly interesting to us, and from now on we will always assume to have chosen values of γ such that $V > V_w^\gamma$.

Note that according to Eq. (9) the crack velocity at the Griffith’s threshold $\delta_G = u_{bk}/\sqrt{3}$ is finite if $u_{bk}/u_{nl} < 2/(\sqrt{3} - 1)$, and is given by

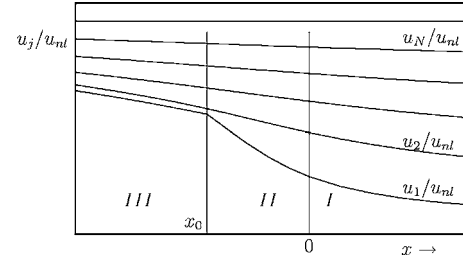


FIG. 3. A case with $N=5$ and δ close to δ_G . For clarity, we only plot the upper half of chains, as the others are symmetric. Only the chain adjacent to the crack, and only in region II, explores the nonlinear regime. As $\delta \rightarrow \delta_G$, $x_0 \rightarrow 0$.

$$V(\delta_G) = V_w \sqrt{1 - \left(\frac{u_{bk}}{u_{nl}} \right)^2 \frac{(\sqrt{3} - 1)^2}{4}}. \quad (14)$$

This is in contrast to cases in which the system is discrete in the direction of crack propagation. In those cases, due to lattice trapping effects the crack cannot propagate if the Griffith’s threshold is not overpassed by a finite amount.

The values in Eq. (9) for the velocity as a function of δ must be compared with the result that is obtained in the absence of hyperelastic effects, namely $V(\delta) = V_w$. The non-trivial result contained in Eq. (9) is a consequence of hyperelasticity in the system. We will see that the same qualitative effects exist in the more interesting cases with $N > 1$.

V. EXACT RESULTS FOR $N > 1$

The previous case $N=1$ is a good starting point in which the analytical solution can be worked out in full detail. But obviously, if we are interested in modeling a macroscopic system we should study the case of a large number of chains.

For $N > 1$ the exact value of the velocity for arbitrary δ cannot be obtained, in general. However, we can provide exact results in some neighborhood of δ_G and δ_U . Consider first the case $\delta \sim \delta_G$. Let us concentrate on one half (the upper one) of the system, since the other is symmetric. Sufficiently close to the Griffith’s threshold, only one chain (the one adjacent to the crack) will enter the hyperelastic state. In this regime the problem can be separated in three regions as shown in Fig. 3. We match the solutions, requiring continuity of the function and derivative of $u_j(x)$, except for the derivative of $u_1(x)$, in which (as in the $N=1$ case) a discontinuity of the derivative of the form (13) exists between regions II and III. The solution obtained will be valid as long as no chain other than the first enters the nonlinear regime and $u_1(x) < u_2(x)$. The width of zone II is determined as part of the solution. The problem stands as a system of $4N+1$ nonlinear algebraic equations, which we solve to any desired accuracy through an iterative method. The results for the velocity are plotted in Fig. 4 as a function of δ/δ_G , and in Fig. 5 as a function of δ/δ_U . We plot data in the full range in which the method is reliable and gives the exact value of the velocity. As it can be observed, the velocity is only weakly dependent on γ (always assuming $V_w^\gamma < V$).

It is interesting to observe from Fig. 4, that even in the limit $N \rightarrow \infty$ our method provides the solution in a finite

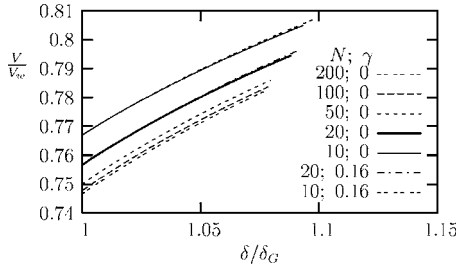


FIG. 4. Analytical results for the velocity vs normalized strain δ/δ_G , for $u_{bk}/u_{nl}=4/3$. It is seen that the dependence on γ is very weak. Through all the range in which we plot the data only chain u_1 (and $-u_1$) explores the hyperelastic regime.

range of δ/δ_G . This means that in all this interval, for a system of infinite chains, there is a single one that explores the hyperelastic regime, and is responsible for the full reduction of the velocity from V_w to the actual value.

In the limit $\delta \rightarrow \delta_G$, we have $x_0 \rightarrow 0$, and region II shrinks to zero. In this limit we obtain the exact values of the velocity and its derivative with respect to δ by solving a linear system of $2N$ algebraic equations. Both $V(\delta_G)$ and $\frac{dV}{d\delta}|_{\delta_G}$ turn out to be independent of γ . From this independence and the scaling form Eq. (3), we can conclude that

$$V(\delta_G, N) = V_w \sqrt{1 - \left(\frac{u_{bk}}{u_{nl}} F_1(N)\right)^2} \quad (15)$$

and

$$\frac{d\sqrt{1 - (V/V_w)^2}}{d\delta} \Big|_{\delta_G, N} = \frac{F_2(N)}{u_{nl}}. \quad (16)$$

The values of the functions F_1 and F_2 for different N are shown in Fig. 6. The limiting value $F_1(N \rightarrow \infty) = 1/2$ can be obtained analytically through an appropriate analysis of the equations in this limit. Extrapolation of the finite N exact values of $F_2(N)$ suggests also that $\lim_{N \rightarrow \infty} (F_2(N)/\sqrt{N/2}) = 1$, but we have not verified it analytically.

We can then write:

$$\sqrt{1 - (V/V_w)^2} \Big|_{\delta_G, N \rightarrow \infty} = \frac{u_{bk}}{2u_{nl}}, \quad (17)$$

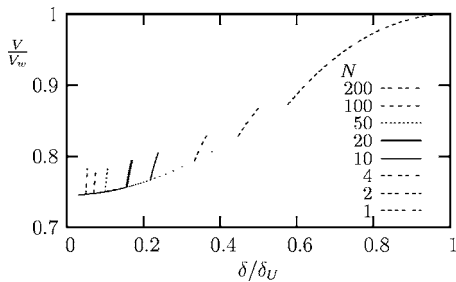


FIG. 5. Same as in Fig. 4, plotted as a function of δ/δ_U , ($\gamma=0$ always).

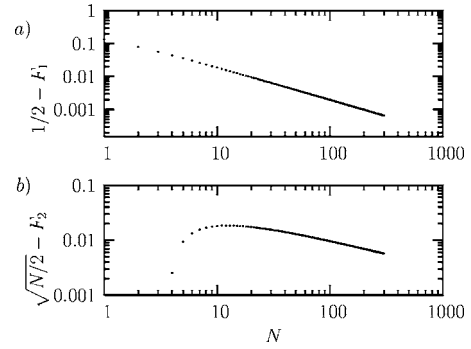


FIG. 6. Plot of the functions $F_1(N)$ and $F_2(N)$ [see Eqs. (15) and (16)].

$$\frac{d\sqrt{1 - (V/V_w)^2}}{d(\delta/\delta_G)} \Big|_{\delta_G, N \rightarrow \infty} = \frac{u_{bk}}{2u_{nl}}. \quad (18)$$

We emphasize again the reduction of the velocity from the value V_w due to the hyperelastic effect. This effect disappears if $u_{nl} \rightarrow \infty$.

A second limiting case can be solved analytically, and that is the asymptotic form of the velocity very close to δ_U . The analysis is based again in matching the solutions of the piecewise linear equation. The situation is sketched in Fig. 7. In region I ($x > 0$) all chains are in the linear regime. In regions II, III, etc., chains enter the nonlinear regime sequentially, starting from the one adjacent to the crack.

When $\delta \rightarrow \delta_U$ (and $V/V_w \rightarrow 1$), it can be seen that the solution of the equations for region II are $N-1$ exponential modes with a diverging decaying constant, and a trigonometric mode with finite frequency. Taking into account that the width of region II (namely $|x_0|$) remains finite even for $V \rightarrow V_w$, we can neglect exponential modes that grow toward negative x . This allows us to obtain the velocity in this limit by solving a system of $2N$ linear equations, matching the solutions between regions I and II only.

The result we obtain is that to lowest order in $\delta - \delta_U$, the velocity can be written

$$\sqrt{1 - \left(\frac{V}{V_w}\right)^2} \Big|_{\delta \rightarrow \delta_U} = \frac{\delta - \delta_U}{u_{nl}} F_3(N), \quad (19)$$

where F_3 is another N -dependent dimensionless function. Note that this result is again independent of γ , and consistent

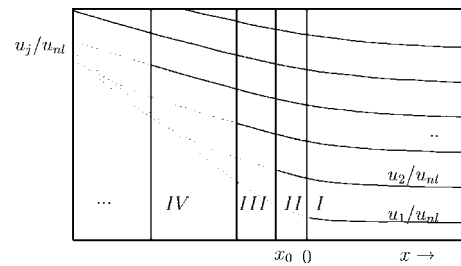


FIG. 7. Sketch of the configuration for δ close to δ_U . In regions I, II, III, etc., we have 0, 1, 2, etc., chains in the hyperelastic regime (dotted lines). The velocity for δ close to δ_U can be obtained analyzing regions I and II only, as explained in the text.

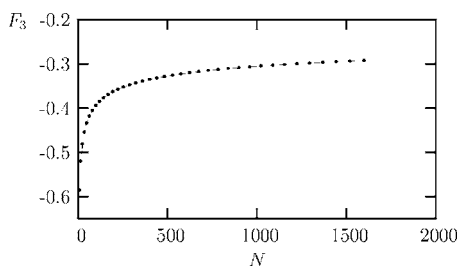


FIG. 8. Dots: Plot of $F_3(N)$ [see Eq. (19)]. Line: fitting of the form $\frac{A}{\log N+B}$ with $A=-3.14$, $B=29.1$. We see that F_3 vanishes as $1/\log N$ for $N \rightarrow \infty$.

with the general expression in Eq. (3). Values of $F_3(N)$ are plotted in Fig. 8. By analyzing in more detail the $N \rightarrow \infty$ limit, it can be shown that F_3 goes to zero as $1/\ln(N)$.

VI. COMPARISON WITH NUMERICAL RESULTS

Although the main results of our work are the analytical findings of the previous section, we include here some results of numerical simulations for two reasons: first of all, some of the results of the previous section are not fully intuitive, and then we think it is clarifying to check them against a numerical simulation. Second, numerical simulations can be done in the full range between $\delta = \delta_G$ and $\delta = \delta_U$, filling the gap between the two analytical limits.

To numerically simulate Eq. (1) we need to discretize the second derivative along x . Introducing a discretization distance ϵ , we arrive formally to an equation that describes a system of point masses coupled by springs both along x and y . The equation is:

$$(\epsilon\rho)\frac{d^2u_{ij}}{dt^2} = \frac{k_0}{\epsilon}[\eta(u_{i+1,j} - u_{i,j}) + \eta(u_{i-1,j} - u_{i,j})] + \epsilon[\nu(u_{i,j+1} - u_{i,j}) + \nu(u_{i,j-1} - u_{i,j})], \quad (20)$$

where η , ν are given in Eq. (2), $(\epsilon\rho)$ is the mass of each point, and ϵ^2/k_0 is the ratio between springs constants connecting particles along vertical and horizontal directions, and it is a measure of the degree of anisotropy of the lattice. For $\epsilon = \sqrt{k_0}$ we have a square lattice, whereas for $\epsilon \rightarrow 0$ we recover the continuous limit of the analytical treatments. As we will see, keeping a finite but small ϵ is also an appropriate form of regularizing the singular results that may appear in the continuum case. We use free boundary conditions in the left border and fixed boundary on the right border of the system. Each time a new vertical spring is broken we shift all coordinates and velocities in such a way that the crack tip remains at the same spatial position in the simulation box.

In Figs. 9 and 10 we present results for $N=1$. They compare very well with the analytical results of the previous section. Note in particular in Fig. 9(b) the oscillation of du/dx for $x < x_0$. This represents the singular behavior of the analytical solution that we have discussed previously. This oscillation is seen in the plot of du/dx , but is hardly visible in the plot of $u(x)$ itself, as its amplitude goes to zero with ϵ . In the case of Fig. 10 we see how the abrupt change on the

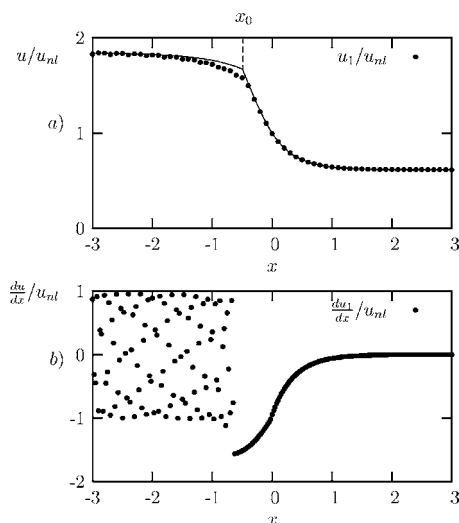


FIG. 9. (a) Analytical (line) and numerical results (points) for $N=1$, $\delta/u_{nl}=1.23$, and $u_{bk}/u_{nl}=2$ ($\epsilon=1/40$ in the numerics). For clarity, only one of every four points of the simulated system is shown. (b) The plot of du/dx , from the simulations. We calculate the derivative in the discrete system for chain j as $du/dx \equiv \frac{u_{i+1,j} - u_{i,j}}{\epsilon}$, where the subindex i is the discretization along the x axis and ϵ is the discretization distance. Note that the only piece of chain in the nonlinear regime is that with $x_0 < x < 0$. The oscillation for $x < x_0$ carries (in the form of kinetic and elastic energy) the excess of elastic energy that is present in the system.

derivative of the analytical solution is very well reproduced in the numerical simulations, supporting the prescription given by Eq. (11). In Fig. 11 we show superimposed analytical and numerical results for $N=20$, for a value of δ in which a single chain explores the nonlinear regime. Again the agreement is very good. Note also in this case the oscillation in du/dx for the first chain behind the crack.

The numerical results for crack velocities are plotted on top of the analytical results in Fig. 12. We see that they agree very well with the analytical values, providing a link between the $\delta \sim \delta_G$ and $\delta \sim \delta_U$ regions.

VII. THE CONTINUOUS LIMIT: $N \rightarrow \infty$

From the finite N results of the previous sections we can try to obtain the behavior of a “macroscopic” material by

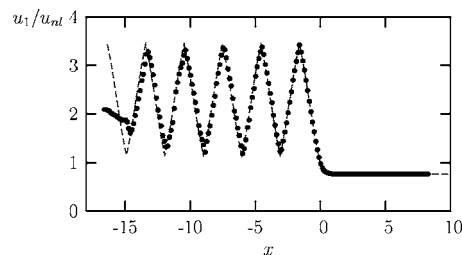


FIG. 10. Analytical (line) and numerical results (points) for $N=1$ with $\delta/u_{nl}=1.53$ and $u_{bk}/u_{nl}=2$ ($\epsilon=1/40$ in the numerics). For clarity, only one every five points of the simulated system is shown. The solution behaves as described in Eq. (10). The numerical results differ at the left border of the system, because the system is finite in the numerical simulation.

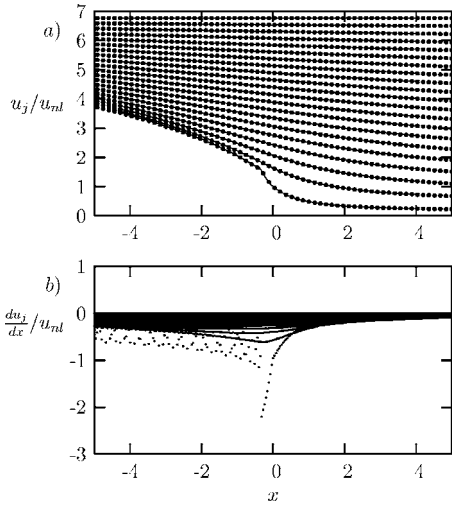


FIG. 11. (a) Analytical (lines) and numerical results (points) for $N=20$, $\delta/u_{nl}=0.33$, and $u_{bk}/u_{nl}=2$ ($\epsilon=1/25$ in the numerics). For clarity, only one every four points of the simulated system is shown. At this strain value only the first chain enters the nonlinear regime. (b) Numerical values of $\frac{du}{dx}$, where the singular oscillation behind the crack is observable.

studying the limit $N \rightarrow \infty$. We must keep in mind however, that the results we are about to discuss still depend strongly on the microscopic details of the model, other microscopic realization giving rise probably to different macroscopic behavior. In fact, we have already emphasized that the fracture of a macroscopic object cannot be described completely in terms of a continuum description, since microscopic details of the breaking process at the crack tip are always relevant. In any case, taking the $N \rightarrow \infty$ limit in our model provides us with one possible realization of a continuum system that we want to analyze now.

The most important quantity we can analyze in the large N limit is the dependence of the crack velocity on the normalized strain δ/δ_G . This is in fact a directly accessible experimental quantity. We already have at hand some analytical results about this [see Eqs. (17) and (18)]. We know the value of V at δ_G (which is strictly lower than V_w), and that of $dV/d(\delta/\delta_G)$ at $\delta=\delta_G$ (which is finite). We also know that

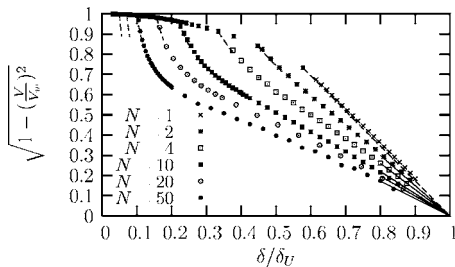


FIG. 12. Numerical results for different number of stripes with $\gamma=0$ and $u_{bk}/u_{nl}=2$. Analytical results close to δ_G are plotted as dashed lines, whereas the analytical asymptotic slopes at δ_U [Eq. (19)] are shown by continuous lines. The agreement is seen to be excellent, considering the discreteness of the numerical model. Note that for the parameters chosen the velocity at δ_G goes to zero when $N \rightarrow \infty$ [Eq. (17)].

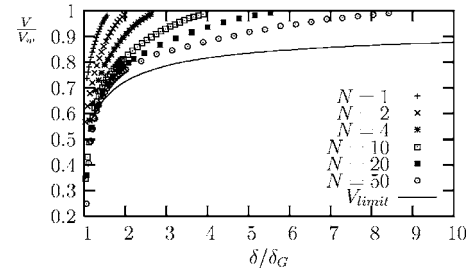


FIG. 13. Same numerical results as in Fig. 12, for different number of stripes with $\gamma=0$ and $u_{bk}/u_{nl}=2$, but plotted as a function of δ/δ_G . The numerical results suggest that, given δ/δ_G , the velocity is a decreasing function of N . This evidence allows us to plot an upper bound (continuous line) for the results in the $N \rightarrow \infty$ case (see the text for details).

eventually V reaches the value V_w for sufficiently large δ/δ_G . But the extremely slow decay with N of $dV/d\delta$ at $\delta=\delta_U$ [Eq. (19)] allows one to infer that $V(\delta/\delta_G)$ will reach the value V_w also very slowly. We present here a nonrigorous argument, which we think reproduces the right tendency. First of all note from the numerical results of Fig. 12 that the asymptotic value of V close to δ_U is a reasonable upper bound for the velocity, i.e., [see Eq. (19)],

$$\sqrt{1 - \left(\frac{V}{V_w}\right)^2} \Big|_{\delta/\delta_G, N} \gtrsim \frac{u_{bk}}{u_{nl}} \left(\frac{\delta/\delta_G}{\sqrt{2N+1}} - 1 \right) F_3(N). \quad (21)$$

On the other hand, when plotted as a function of δ/δ_G (Fig. 13), the numerical results suggest that, for a fixed value of δ/δ_G , the velocity is a decreasing function of N . We think this is rigorous result, although we do not have a proof of it. Accepting this statement as valid, we can obtain an upper bound for the velocity in the $N \rightarrow \infty$ limit by maximizing the right-hand side of Eq. (21) with respect to N for each value of δ/δ_G . The result is plotted in Fig. 13 as a continuous line. For large δ/δ_G , the leading analytical form can be obtained as follows:

$$V(\delta/\delta_G, N) \Big|_{N \rightarrow \infty, \delta/\delta_G \rightarrow \infty} \sim V_w \left[1 - \alpha \left(\frac{u_{bk}}{u_{nl}} \frac{1}{\ln \delta/\delta_G} \right)^2 \right], \quad (22)$$

where α is a numerical constant. This is in fact an extremely slow convergence to the limiting value V_w . We think this is a very important result. It tells that strictly speaking, hyperelastic softening does not reduce the limiting value of the velocity for sufficiently large applied strain. However, in view of its extremely slow convergence to this limit, from a practical point of view we can say that hyperelastic softening produces an appreciable reduction of the limiting velocity. In particular, we see that this reduction of the velocity does not exist when hyperelasticity is absent (namely, for $u_{nl} \rightarrow \infty$).

VIII. DISCUSSION AND CONCLUSIONS

We have analyzed the effect of hyperelastic softening in a model of crack propagation in a stripe geometry under mode

III fixed displacement boundary conditions. The model is continuous in the propagation direction and has a finite number of chains in the perpendicular direction. The two central chains of the stripe can decouple when they separate more than a critical distance u_{bk} , generating a crack in the model.

In the case in which the chains are perfectly harmonic the velocity of crack propagation is equal to the wave velocity V_w in the full range of external strain δ between the Griffith's threshold δ_G and the strain of uniform breakdown δ_U .

We have studied how this result is affected by the inclusion of hyperelastic softening in the chains, namely, a softening of the spring constant of the chains when the stretching is greater than a threshold value. We have provided analytical results in some cases, and complemented them with numerical simulations.

For the case of a single chain the full analytical solution has been worked out. It is clearly seen already in this simple case that hyperelastic softening reduces the velocity from the harmonic case. Now the velocity has a nontrivial dependence on δ , and becomes equal to V_w only at δ_U .

We have given the analytical solution for the velocity in neighborhoods of $\delta = \delta_G$ and $\delta = \delta_U$. The main results in this case are the following. The crack velocity at δ_G is strictly lower than V_w . It decreases as a function of the number of chains but may well be finite in the $N \rightarrow \infty$ limit for some range of the parameters of the model. There is a finite range of δ/δ_G in which only the chain adjacent to the crack enters the hyperelastic regime. This range remains finite for large N . This means that our analytical treatment provides the exact value of the velocity in a finite range around $\delta/\delta_G = 1$ even in the $N \rightarrow \infty$ case.

The crack velocity tends always to V_w when $\delta \rightarrow \delta_U$. In the large N limit this can be stated as the fact that V tends to V_w for $\delta/\delta_G \rightarrow \infty$. However, our estimations show that this convergence is very slow, namely like $\sim 1/\ln^2(\delta/\delta_G)$.

ACKNOWLEDGMENT

The authors acknowledge the financial support of CONICET (Argentina).

-
- [1] L. B. Freund, *Dynamic Fracture Mechanics* (Cambridge University Press, Cambridge, 1990).
 - [2] K. B. Broberg, *Cracks and Fracture* (Academic Press, San Diego, 1999).
 - [3] J. Fineberg and M. Marder, *Phys. Rep.* **313**, 1 (1999).
 - [4] E. Sharon and J. Fineberg, *Nature (London)* **397**, 6717 (1999).
 - [5] D. A. Kessler and H. Levine, *Phys. Rev. E* **68**, 036118 (2003).
 - [6] L. I. Slepyan, *Sov. Phys. Dokl.* **26**, 538 (1981); **37**, 259 (1992).
 - [7] J. Buehler, F. F. Abraham, and H. Gao, *Nature (London)* **426**, 141 (2003).
 - [8] T. M. Guozden and E. A. Jagla, *Phys. Rev. Lett.* **95**, 224302 (2005).